Egyptian Geophysical Society
EGS Journal, Vol. 11, No. 1, 105-119 (2013)

RESERVOIR CHARACTERIZATION OF THE LOWER MIOCENE SEDIMENTS, CENTRAL TROUGH OF THE SOUTHERN GULF OF SUEZ, EGYPT

M.S. El Sharawy

Geophysical Sciences Department, National Research Centre, Cairo, Egypt.

خصائص خزان رواسب متكون النخل – أسفل الميوسين – بالمنخفض المركزي بجنوب خليج السويس – مصر.

الخلاصة: يعتبر متكون النخل – أسفل الميوسين – منتجا للنفط في العديد من حقول النفط بخليج السويس سواء من خلال الرسوبيات الرملية او من خلال الحجر الجيري. تم اختيار ستة آبار بجنوب خليج السويس لدراسة جيولوجية و بتروفيزيقية متكون النخل الذي يتكون أساسا من عضو شعب علي لأسفل و عضو متبخرات غارة لأعلي. وجد أن المتكون الكامل يوجد عادة علي الرمية السفلية بينما غالبا ما يوجد بشكل غير كامل علي الرمية العلوية. مرجع ذلك لحركة الفوالق التي اعقبت ترسيب عضو شعب علي. كما أمكن تقسيم عضو شعب علي إلي ثلاث وحدات صخرية كل وحدة تمثل تركيب صخري وبيئة ترسيبيه مختلفة عن الأخري. يمثل الحجر الرملي لعضو شعب علي خزان جيد إلي ممتاز من حيث الخصائص البتروفيزيقية حيث يتميز بنفاذية ومسامية عالية بالإضافة إلي محتوي طفلي ضئيل. أمكن من خلال الدراسة أيضا – تحديد ثلا ث أنواع صخرية وتسع وحدات تدفق هيدروليكيه.

ABSTRACT: *The Lower Miocene Nukhul Formation is oil producing in several fields throughout the Gulf of Suez either from clastics or reefoidal limestones. Six wells were selected in the central trough of the southern Gulf of Suez to investigate the geologic and petrophysical properties of the Nukhul Formation. It consists mainly of lower Shoab Ali clastics Member and upper Ghara anhydrite Member. The complete succession of the Nukhul Formation is usually encountered on the downthrown side and faulted part is usually located on the upthrown one. This may be attributed to fault movements post Shoab Ali Member. This member can be divided into three units. The upper boundary of the lower unit defined a sequence boundary. The middle unit represents a sandstone interval deposited in a basin floor fan. The upper unit which its lower boundary defined as an erosion surface was deposited in a fan complex. The Nukhul clastics represent a good reservoir quality with high porosity and permeability as well as low shale content. Three reservoir rock types as well as at least nine hydraulic flow units can be detected within these Nukhul clastics.*

INTRODUCTION

The Nukhul Formation represents the first clue to the Gulf of Suez rifting. However, initiation of the Gulf of Suez rifting was started earlier during the Late Oligocene (Garfunkel and Bartov, 1977). The depositional facies and thickness of the Nukhul Formation and the overlaying sediments were controlled in most part by the degree of the rift intensity. Other controlling factors include tectonic elements (uplift or subsidence), climate, sea level change, sediments supply and phyisographic position of the depositional basin. Several studies were published concerning with the Gulf of Suez tectonic evolution, structure setting, stratigraphy and the petroleum potentiality by Garfunkel and Bartov, 1977; Evans, 1988; Montenat et al., 1986; 1988; 1998; Richardson and Arthur, 1988; Patton et al., 1994; EGPC, 1996; McClay et al., 1998; Plaziat et al., 1998; Bosworth et al., 1998; Bosworth and McClay, 2001;Winn et al., 2001; Moustafa, 2002; Jackson et al., 2006 and Wilson et al., 2009.

The syn - rift strata was subjected to various divisions and nomenclatures. The Egyptian General Petroleum Corporation (EGPC) Stratigraphic Committee (1964) divided the Miocene sediments of the Gulf of Suez into two groups: Ras Malaab Group (Evaporite) that overlies the Gharandal Group (Clastic). The last group is often dated as Lower and Middle Miocene, while the Ras Malaab Group is belonging to the Middle/Upper Miocene. For petroleum geologists, Gharandal Group has a significant role in forming petroleum reservoirs, and many of its units are significant as source rocks. The evaporites of Ras Malaab Group are always thought as the ultimate seal. Generally, the thickness of the two groups is about twice that of the pre- Miocene sequence. However, in the depocenters the thickness of the two groups is five times more than that of the Pre- Miocene sequence reflecting a rapid sediment accumulation and a fast subsidence during a relative short geologic time (El Sharawy, 2006).

The syn - rift megasequence was divided by Montenat et al. (1986) into 4 groups, namely; A, B, C and D from base to top. Each group is limited by an angular discordance of regional extension, which seems to reflect the major stages of the rifting. Plaziat et al. (1998) adopted Montenat such classification but subdivided each group into units (Table 1).

Dolson et al. (1996) divided the Miocene deposits of the northern Gulf of Suez into five regional terraces defined time breaks and the intervening units were treated as “sequence”, while Ramzy et al. (1996) recognized at least seven terraces in the central and southern Gulf of Suez.

Study area and data:

Six wells distributed throughout the central trough of the southern Gulf of Suez were selected to study the geologic and petrophysical attributes of the Nukhul Formation. The selected wells are belonging to four oilfields which are from South to North; Ashrafi, Hilal, Sidki and Amal (Fig. 1). The first three oilfields are produced from Miocene and Pre Miocene reservoirs. The fourth field (Amal) is produced only from Miocene reservoir.

Table 1: Classification and nomenclature of syn – rift megasequence (Age after Patton et al., 1994).

Epoch	Age	Classification				
		EGPC, 1964		Montenat et al., 1988	Palziat et al., 1998	Ramzy et al., 1996
Pliocene			Post – Miocene deposits	D	D	
Miocene	Messinian	Ras Malaab Group	Zeit	C	C2	
	Tortonian		South Gharib			
	Serravallian		Belayim		C1	S50
		Gharandal Group	Kareem		B3	S40
	Langhian		Upper Rudies	B	B2	S30
	Burdigalian		Lower Rudeis		B1	S20
	Aquitanian to Early Burdigalian		Nukhul	A	A2	S10

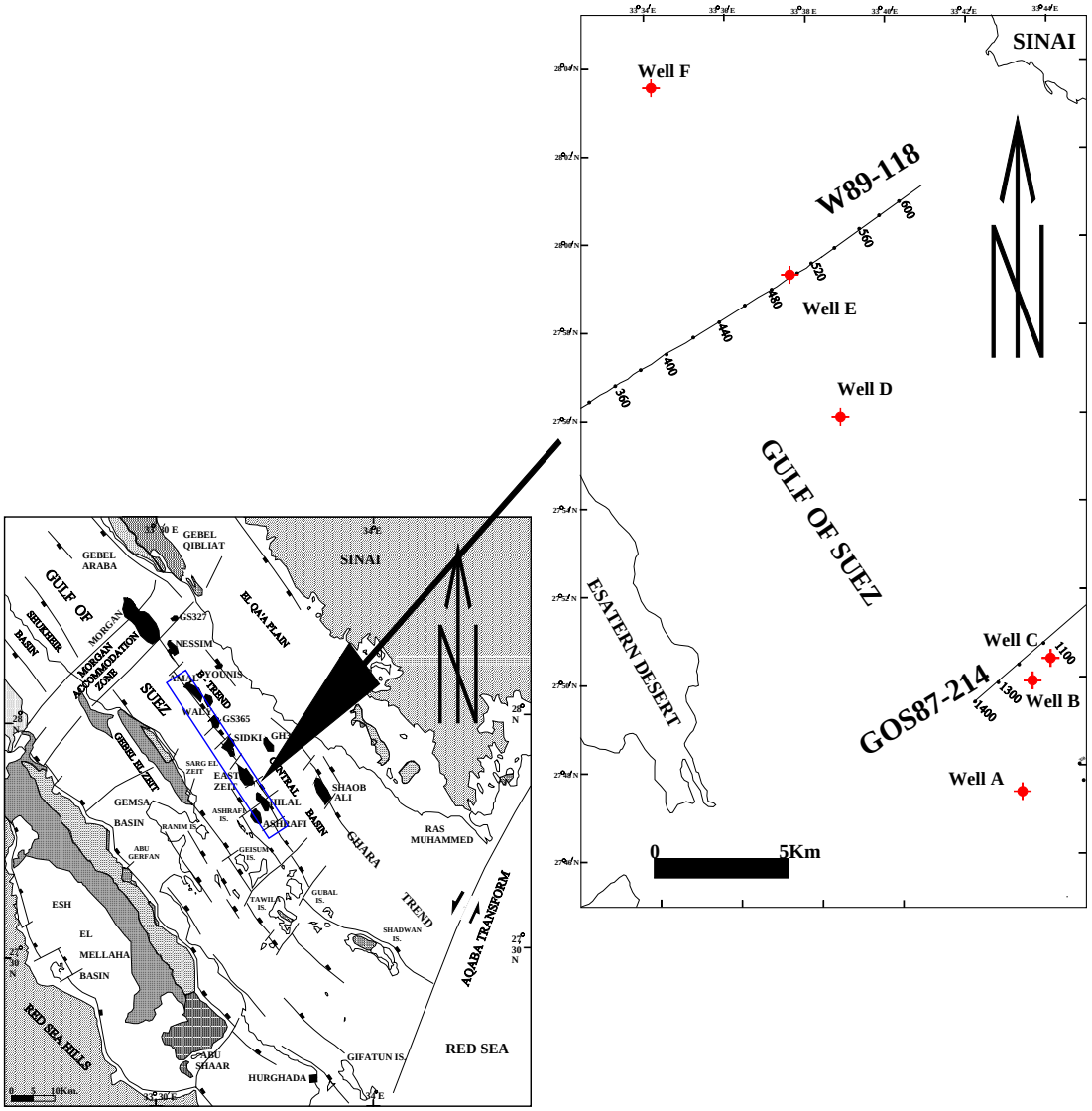

Fig. (1): Location map of the study area (modified after Bosworth et al., 1998).

The available data include electric logs, routine and special core analysis as well as 2D seismic profiles. The electric logs include gamma ray, natural gamma ray (wells A and F), density, neutron, sonic, resistivity, dipmeter and composite. The routine core analysis was available for wells (A and B). Such core analysis includes horizontal and vertical permeability, helium and fluid porosity, grain density and fluid saturation.

In well A, one core plug (3 ft thick) was analyzed provided three core samples. The horizontal permeability ranged from 1257 to 2468 md with average value of 1993 md. The helium porosity ranged from 27.6% to 29.8% with average value of 28.6%. The grain density has 2.65 g/cc average value. The core analysis indicates that the sandstone is tansh grey fine to medium grained occasionally coarse – grained with traces of glauconite and pyrite.

In well B, three core plugs (81 ft thick) were analyzed provided 81 core samples. The uppermost six samples are siltstones and the remaining samples are sandstones. The horizontal permeability ranged from 0.93 to 4020 md with average value of 1118 md. The helium porosity ranged from 9.4% to 22.9% with average value of 17.7%. The grain density has 2.65 g/cc average value. The core analysis indicates that the sandstone is light grey medium to coarse grained occasionally fine – grained with mica and iron oxides, traces of glauconite, kaolinite patches, argillaceous cement and poor to medium cemented.

The special core analyses (SCAL) are available for wells A and B. They provide determination of cementation and saturation exponents and formation factor. Eight core samples in well B were subjected to mercury injection provided eight mercury injection capillary pressure curves from which the pore throat size and the best relation between permeability, porosity and pore throat size can be determined.

METHODOLOGY

To achieve the purpose of this article, electric logs were environmentally corrected and depth matched with core data. The IP software program was used to calculate the petrophysical parameters such as effective porosity, water saturation and clay volume. 10%, porosity, 35% clay volume and 50% water saturation are used as cutoffs. The cementation factor, saturation exponent and formation water resistivity derived from SCAL are introduced to IP to calculate such petrophysical parameters. Dipmeter in cluster processing is used to define the components such as faults and unconformities. Determination of sequence stratigraphic boundaries is defined based on Neal et al. (1993) contributions.

Nukhul formation:

A wide variation in depositional facies characterized the Nukhul Formation. The facies changed from clastics sandstone, conglomerates and shale to carbonates and evaporites. Due to these wide lithofacies variations, Souadi and Khalil (1984) subdivided the Nukhul Formation into lower clastic Shoab Ali Member occurred only in the southern Gulf of Suez and three coeval members. Ghara Member occurs only in the southern Gulf of Suez and consists of anhydrite and marl. October Member consists of sandstone and conglomerates and occurs in the northern Gulf of Suez. Hydrocarbons can be produced from many oilfields such as Asl, Sudr and Matarma. Gharamul Member consists of reefoidal limestones which produced oil from several fields e.g. Esh – El Mellaha and Issran (EGPC, 1996).

Another comprehensive study of the Nukhul Formation was introduced by Winn et al. (2001). They divided the Nukhul Formation at Gebel Zeit into two units. Lower marine clastic unit was deposited by sediments gravity flows where water depth was more than 300 ft. Upper carbonate unit, in response to the sea level rise, consists of dolomite and calcareous dolomite deposited in deep open marine condition. They stated that deposition during the Nukhul Formation was controlled by short – segments, closely spaced faults.

In the study area, the Nukhul Formation rested unconfromably on the Eocene deposits or older rocks and is overlain by the Rudeis Formation (Fig. 2). The complete section was encountered in well C. In other wells, missed sections are detected from well – to – well correlations (Fig. 3). The thickness ranged from 568 ft in the South to 192 ft thick in the North (Table 2). The Nukhul Formation can be divided from top to bottom into;

1- Nukhul paleo:

The Nukhul Paleo unit represents the uppermost part of the Nukhul Formation. It consists mainly of shale and limestone intercalations. The thickness varies from 15 ft in well E to about 180 ft in well A (Table 2). The Nukhul paleo is absent in well B.

2- Ghara member:

The Ghara Member consists of intercalations of anhydrite, shale, limestone and marl. The anhydrite can be completely absent as in well A, occurred in one layer as in well E or occurred in two layers as in wells B and C. The anhydrite layers were separated by open to shallow marine facies. These anhydrite layers may be represented fall in the sea level at the end of Aquitanian (Haq et al., 1987). The thickness of the anhydrite layers vary from one well to another. In well B, the upper layer attains 60 ft thick while the lower layer attains about 22 ft thick. In well C, the upper layer is 6 ft thick while the lower layer is 10 ft thick. In well F, both anhydrite layers have similar thicknesses with 23 ft thick for each. The thickest section was encountered in well D in which 216 ft thick were drilled. It consists of two layers of anhydrite separated by about 170 ft thick of marl. The thickness of anhydrite layers ranged from 20 to 26 ft. The Ghara thickness decreased northwards to 117 ft thick as in well F.

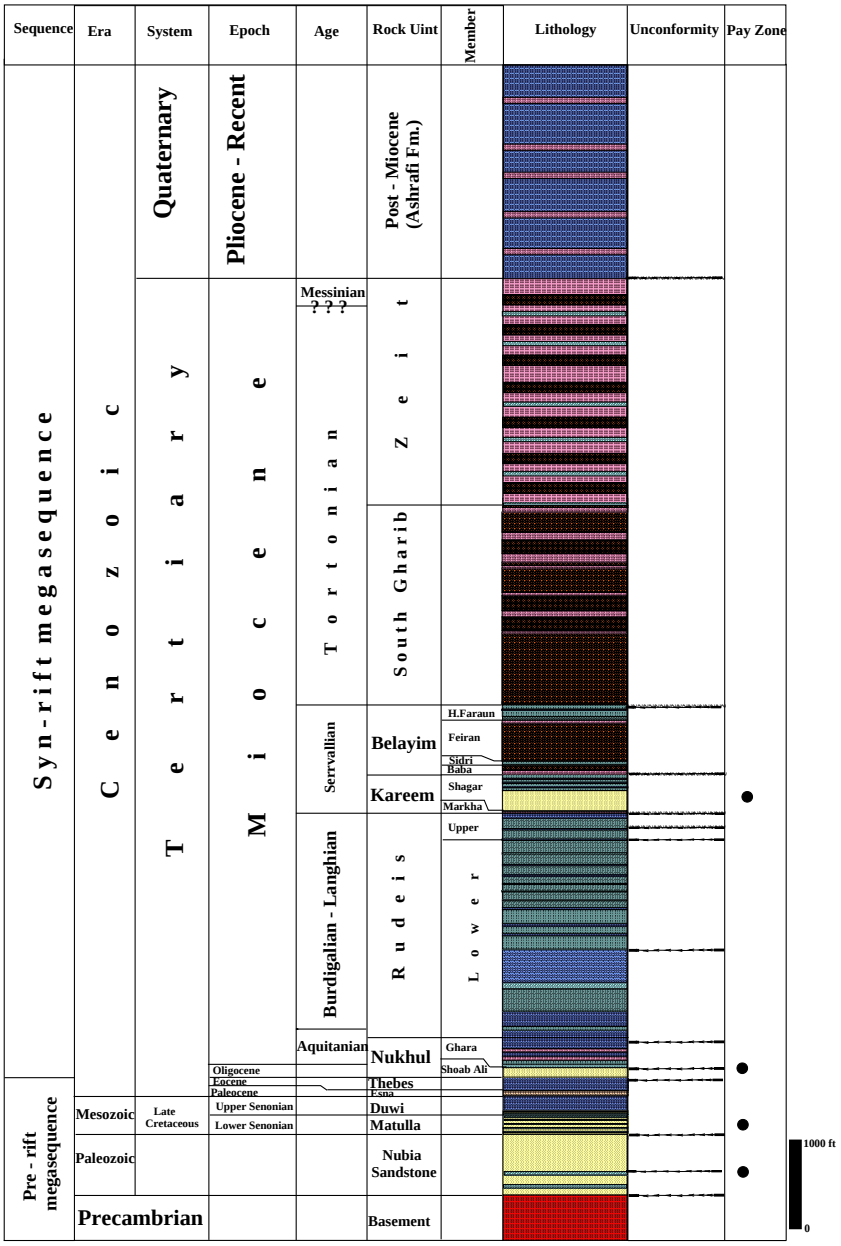

Fig. (2): Generalized stratigraphic column for the central trough of the southern Gulf of Suez (Rock Units age after Patton et al., 1994).

Table 2: Nuhkul Formation thickness (ft) in the studied wells

Well	Total	Paleao	Evaporite	Clastics
A	568	187	174	207
B	378	-	109	269
C	541	139	170	232
D	258	42	216	-
E	223	15	208	-
F	192	75	117	-

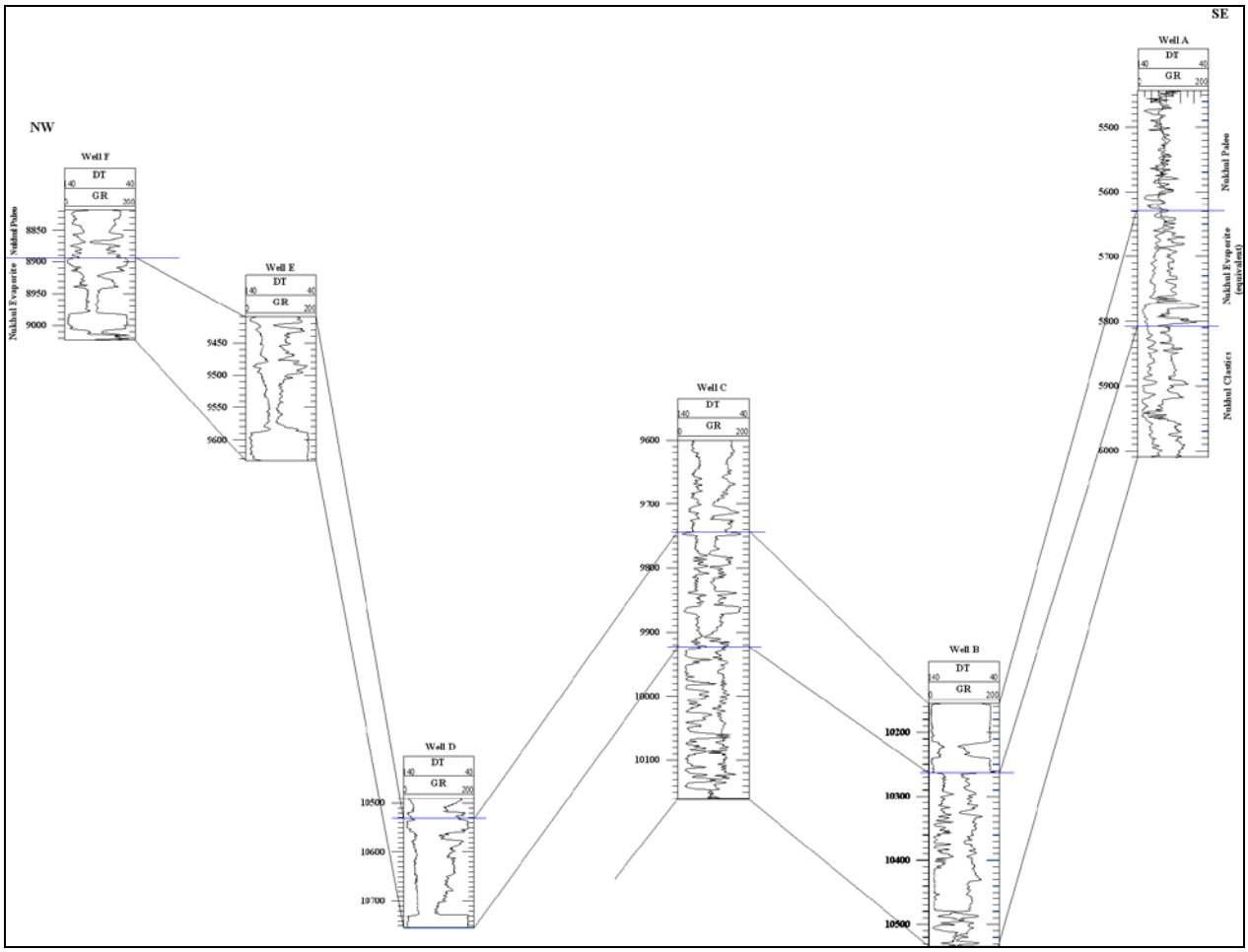

Fig. (3): Well – to – well correlations showing the missed sections in the Nukhul Formation.

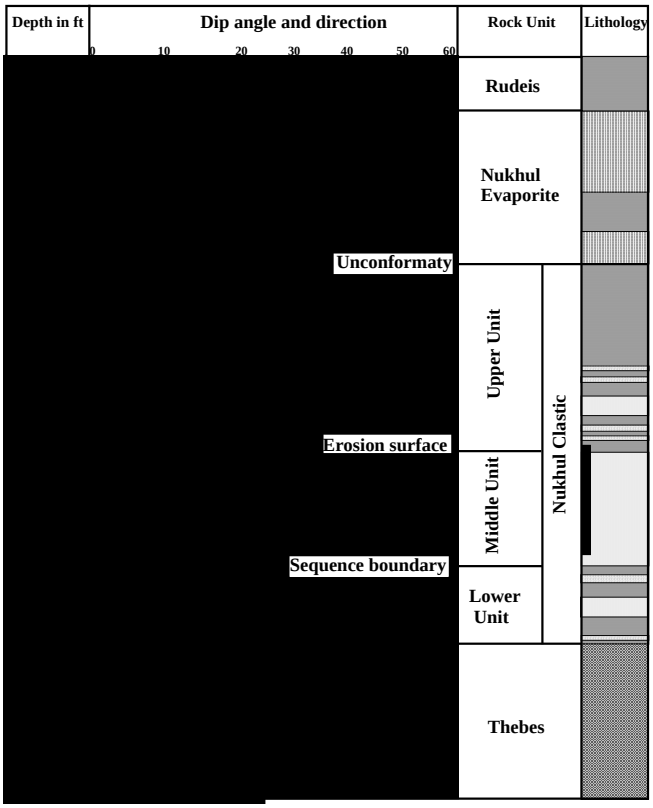

Fig. (4): Dpmeter log in well B.

3- Shoab Ali Member:

The Shoab Ali Member consists of intercalations of sandstone and shale. The thickest section was encountered in well B in which 269 ft thick of sandstone and shale with gross sand of 131 ft rested unconformably on the Thebes Formation were encountered. This member can be subdivided into three units. The upper unit consists of shale and sandstone intercalations. The sandstone ratio increased downwards. The thickness is 132 ft. The middle unit consists of 82 ft thick of sandstone rested unconformably on the lower unit and overlain unconformably by the upper unit as indicated from dipmeter (Fig. 4). The lower unit consists of intercalations of sandstone and shale. It attains 55 ft thick.

RESULTS AND DISCUSSIONS

Six drilled wells, distributed along the southern Gulf of Suez, were selected to study the Nukhul Formation. Three of them were encountered the Shoab Ali Member. These wells are A, B and C. Absence of the Shoab Ali Member in other wells is attributed to faulting processes (Fig. 5).

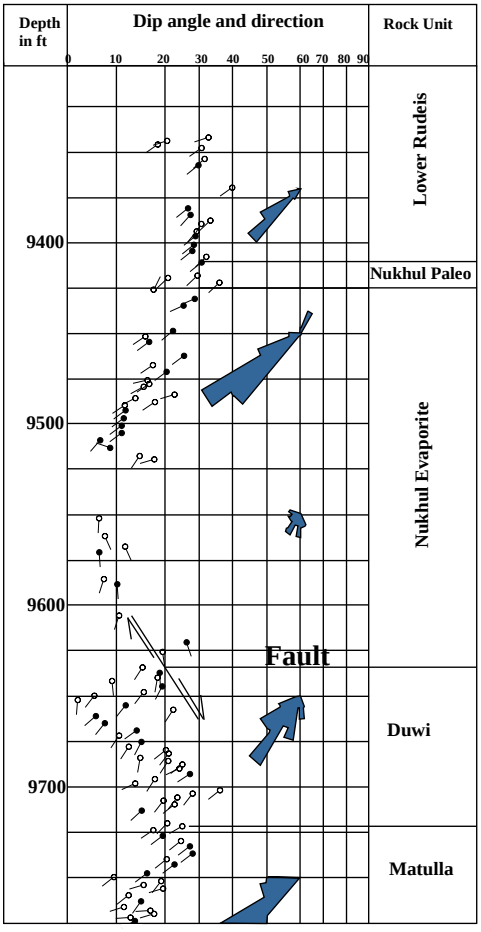

Fig. (5): Dipmeter of well E indicates that missing Nukhul clastic is due to normal fault.

The well drilled on the downthrown side encountered the complete Nukhul Formation (Fig. 6).

In contrast, the well drilled on the upthrown side mostly missed the Shoab Ali section (Fig. 7). So, the movements along the Gulf of Suez fault trends were initiated after deposition of Shoab Ali Member and continued during deposition of the Ghara one. These movements resulted in creation of large antithetically tilted blocks (Montenat et al., 1998). The Shoab Ali Member can be divided into three units based on lithology. Upper and lower units are characterized by intercalations of shales and sandstones. The middle unit consists mainly of sandstone. The sandstone of the middle unit may be deposited in basin floor fan as indicated from the response of electric logs (blocky gamma ray character with sharp base). The typical basin floor fan can be observed in well B between 10410 and 10479.5 ft depth. This interval is characterized by high porosity and permeability and low clay content. The upper unit, which its lower boundary is characterized by erosion, may be deposited in slope fan complex where sands were deposited as overbank sheets and alternate with shale. The lower unit may be deposited in a highstand system tract as indicated from the electric log and the nature of sediments. Sequence boundary separated the lower unit from the middle unit (Fig. 4).

Plotting of potassium versus thorium indicates that most of the clays are kaolinite with traces of heavy minerals (Fig. 8). The well log interpretation indicates good reservoir quality in which the litho – saturation crossplots at wells A, B and C reveal low shale volume, low water saturation and high porosity (Figs. 9, 10 and 11).

Good empirical relation exists between core porosity (Φc in %) and core permeability (Fig. 12). The relation can be expressed in the following equation with a coefficient of determination $(r^2) = 0.85$:

$$K = 0.017\, e^{0.553\,\Phi c} \qquad (1)$$

This good relation between permeability and porosity is rarely encountered. This may be attributed to the following reasons. First, deposition in a basin floor fan gives excellent reservoir properties. Second, low shale content and low to medium cementation resulted in low reduction in original porosity and permeability and consequently the porosity plays the major role in determination of permeability.

Permeability can be predicted using electric logs via several methods such as empirical equations (Morris and Biggis, 1967 and Timur, 1968). It can be predicted also using statistical methods such as regression analysis and artificial neural network. Based on irreducible water saturation derived from capillary pressure, the Timur equation has the following form with $r^2 = 0.87$:

$$K = 0.00007\, \Phi^{3.9} Swir^{1.9} \qquad (2)$$

It is noticed that the exponents are close to that of Timur equation (4.4 and 2). However, in this equation there is an irreversible relationship between permeability and irreducible water saturation.

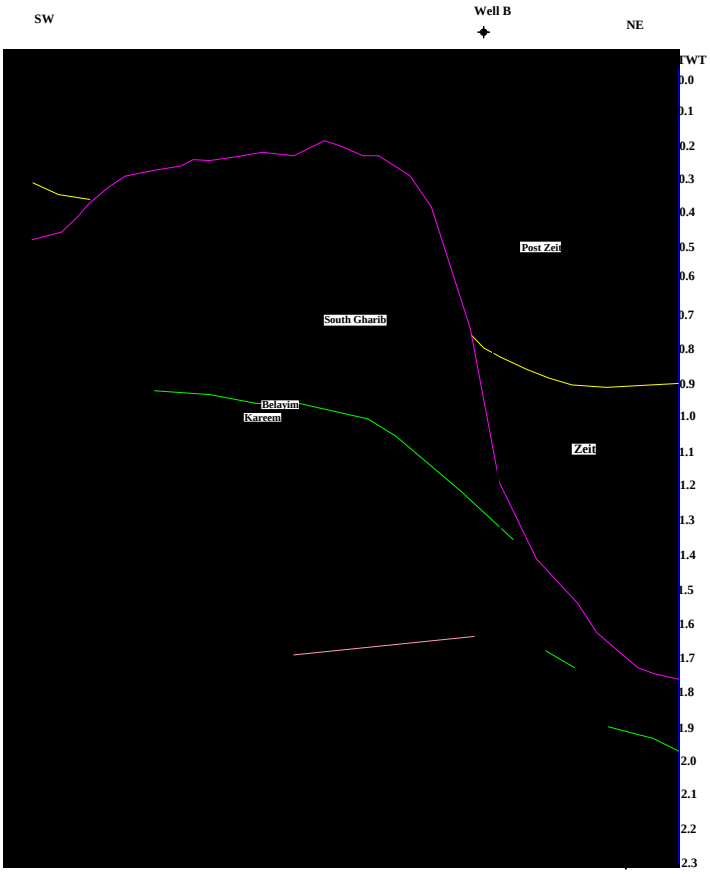

Fig. (6): Seismic line GOS 87 -214 interpretation showing location of well B on the downthrown side.

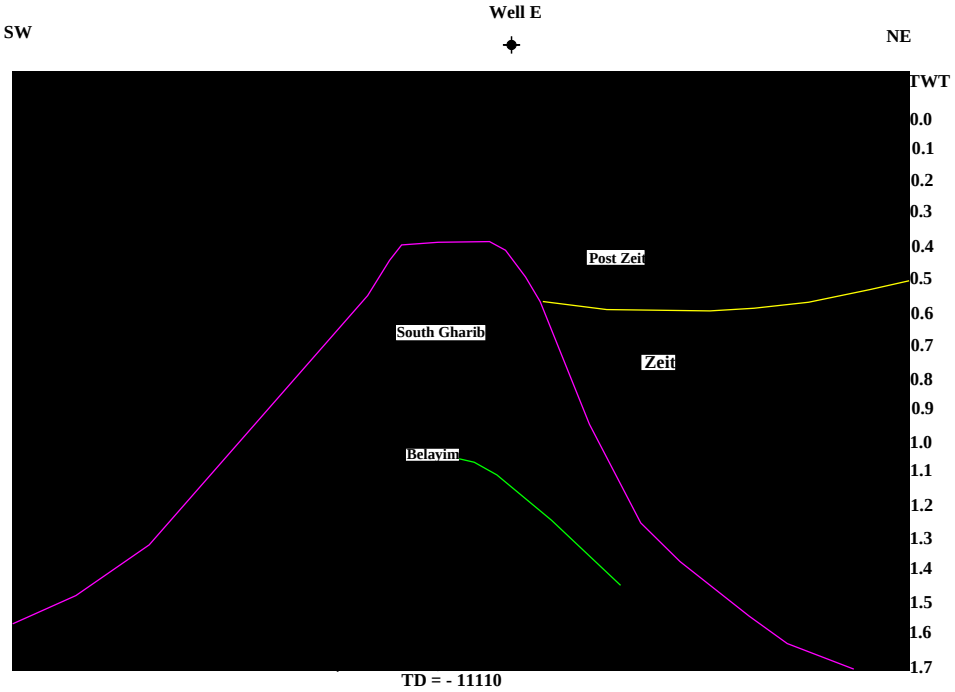

Fig. (7): Seismic line W89 -118 interpretation showing location of well E on the upthrown side.

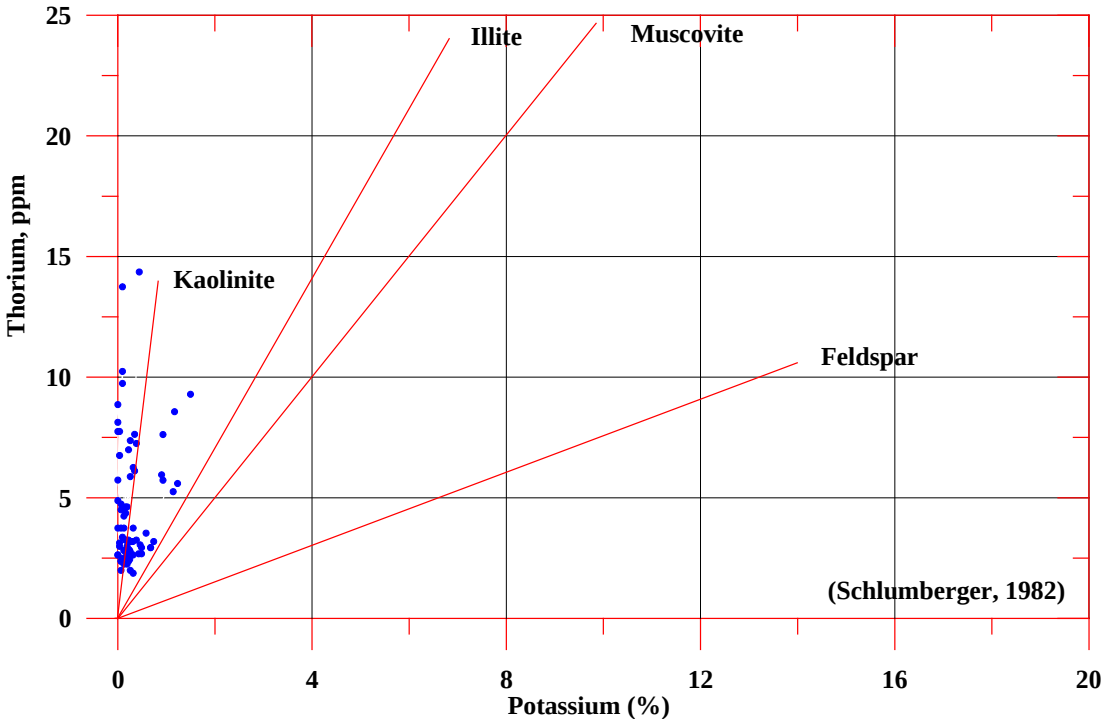

Fig. (8): Identification of clay minerals from potassium versus thoruim crossplot in well B (Schlumberger, 1982).

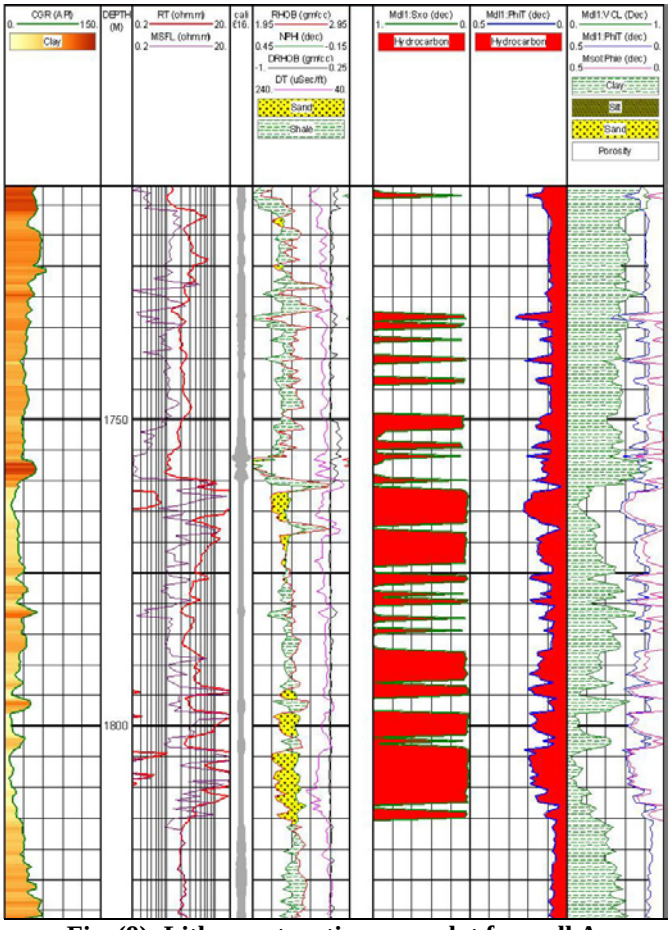

Fig. (9): Litho – saturation crossplot for well A.

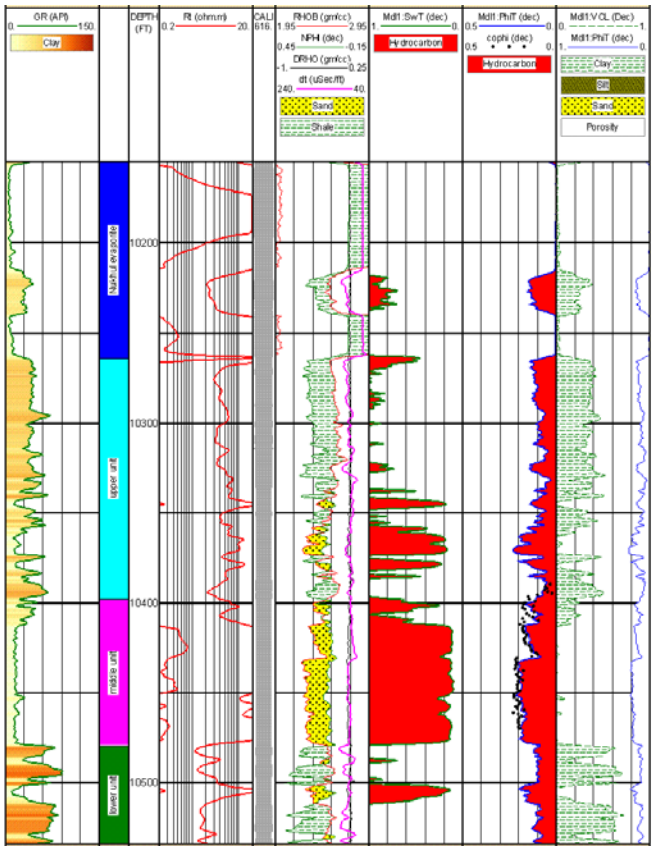

Fig. (10): Litho – saturation crossplot of well B.

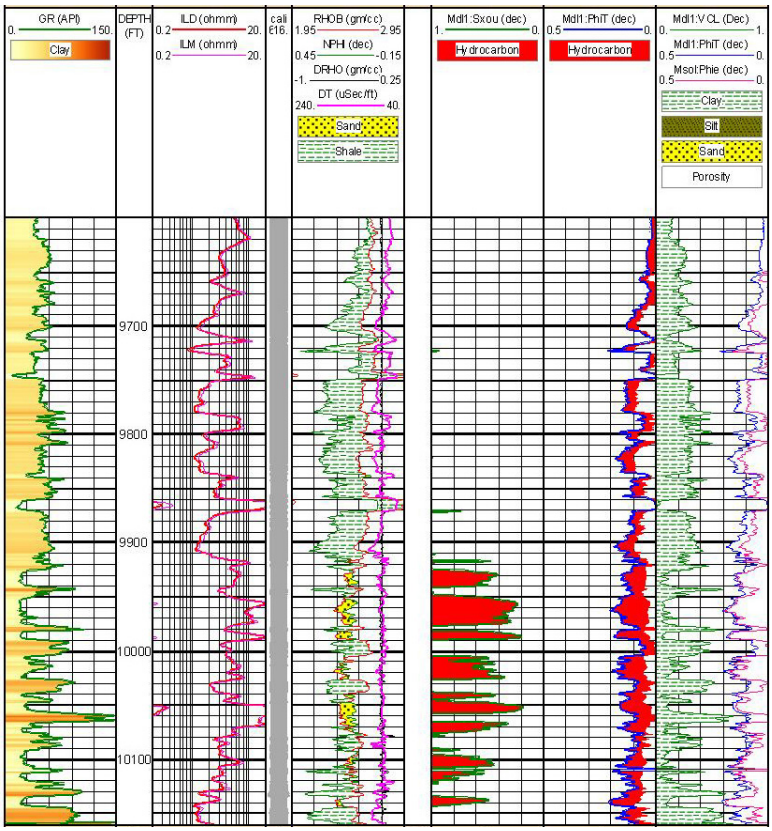

Fig. 11: Litho – saturation crossplot for well C.

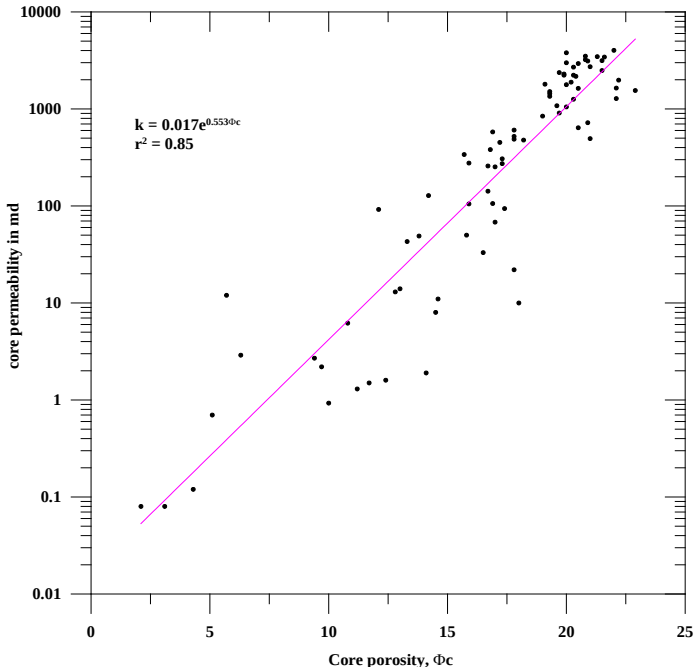

Fig. (12): Core permeability versus core porosity in well B.

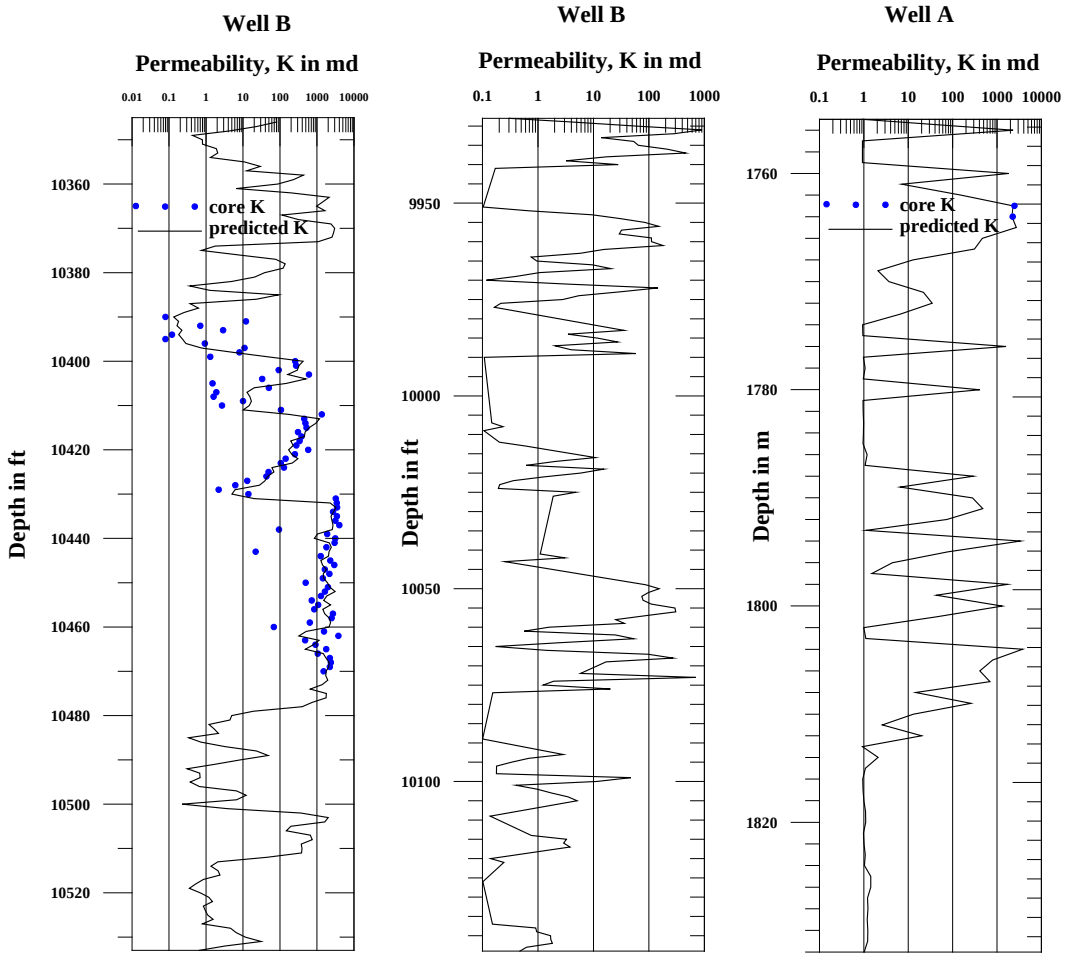

Fig. (13): Predicted permeability using artificial neural network for Nukhul clastics.

Good relation can be observed between permeability and density log. The relation has the following form with r^2 =0.716:

$$\ln K = -23.22\ \rho_b + 60.116 \qquad (3)$$

However by using Multiple Regression Analysis, it gives weak relation. Using artificial neural network, the permeability prediction improved considerably (Fig. 13). The prediction was based on Φn, ρ_b and Φe as input and permeability as output. The relation between core porosity (Φc) and log – derived porosity (Φd) can be expressed as the following with r2 = 0.753:

$$\Phi c = 0.0687 + 0.7119\ \Phi d \qquad (4)$$

Using regression analysis improves the relation slightly with r^2 = 0.79:

$$\Phi c = 1.13 - 0.406\ \rho_b \qquad (5)$$

Heterogeneity of the Nukhul reservoir can be determined based on two scales; pore scale and macro scale. Respecting to pore scale and depending on Dykstra - Parsons Coefficient (Vk) (1950), the Nukhul clastics are extremely heterogeneous where Vk = 0.98 (Fig. 14). Heterogeneity based on macro scale can be observed from intercalations of sandstone and shale, missed sections and effect of faults and unconfromaties.

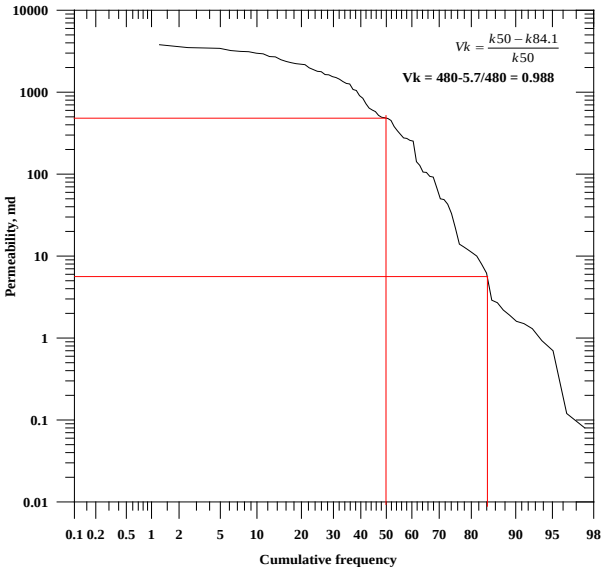

Fig. (14): Determination of reservoir heterogeneity using Dykstra - Parsons Coefficient, Vk.

Anisotropy greatly affects fluid flow characteristics of the rock. The difference in permeabilities measured parallel and vertical to the bedding plane is the consequence of the origin of the sediment. It is a measure of the variations of physical properties in the horizontal and vertical directions, which contributes to the variations of cementation exponent "m " (Salem and Chilingarian, 1999). It is expressed in terms of the hydraulic anisotropy coefficient "λ_h" as follows:

$$\lambda_h = \left(\frac{K_h}{K_v}\right)^{\frac{1}{2}} \qquad (6)$$

Where: K_h and K_v are the horizontal and vertical permeabilities respectively, parallel and normal to the bedding planes. The hydraulic anisotropy coefficient increases with increasing the horizontal permeability along the bedding planes. The horizontal permeability is always greater than the vertical one, unless the medium is completely isotropic. Anisotropy normally ranges between 1 and 5. In the Nukhul Formation, anisotropy is ranged from 0.26 to 6.43 with average value of 1.36 (Fig. 15).

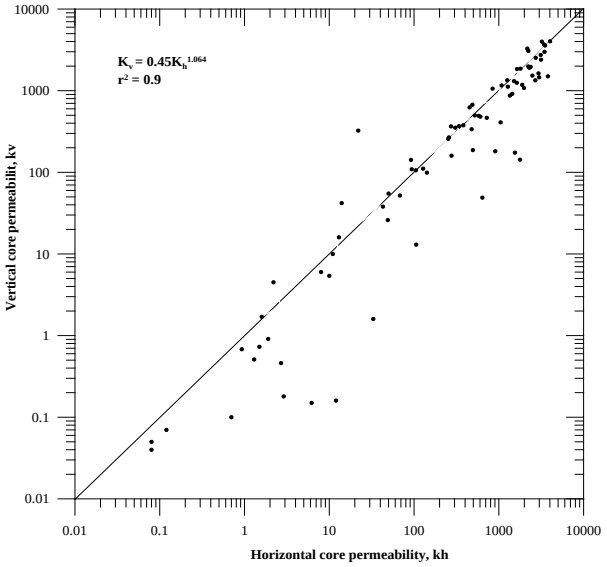

Fig. (15): Vertical permeability versus horizontal permeability showing the Nukhul reservoir anisotropy.

Hydraulic Flow units can be determined from Stratigraphic Modified Lorenz plot (SML) or Winland equation. Gunter et al. (1997) described a technique for combining porosity, permeability, and bed thickness data for flow unit identification. They utilized the Stratigraphic Modified Lorenz plot for characterization. The SML plot is a crossplot of "cumulative flow capacity" – defined as the product of average permeability time thickness of an interval (kh) – versus "cumulative storage capacity" – defined as the product of average porosity and thickness of the same interval (Φh). Change in the slope indicates a new flow unit while horizontal trend can be treated as barrier where no flow occurred. Figure16 shows the SML plot for well B. We can determine at least nine HFU in well B for the cored interval with six barriers. We can conclude that about 90% of the fluid flow has been occurred from the interval between 10430 and 10470 ft depth (Fig. 17). This figure indicates also high degree of heterogeneity in this well. The mercury injection capillary pressure curves indicate three hydraulic flow units for these eight samples (Fig. 18). The HFU1 represents gentle plateau indicating narrow pore throat size distributions (well sorted). On the other hand,

HFU3 represents steep plateau indicating wide pore throat distributions (poorly sorted).

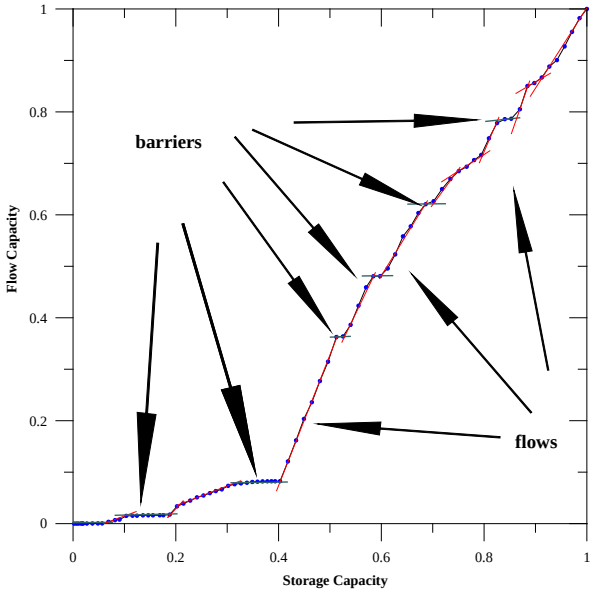

Fig. (16): Stratigraphic modified Lorenz (SML) plot showing the hydraulic flow units in the Nukhul Formation at well B.

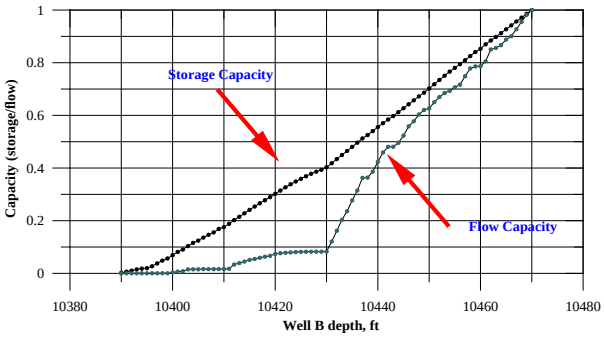

Fig. (17): SML plot showing reservoir flow and storage capacity for well B. We note that 90% of the productions come from the interval between 10430 and 10460 ft depth.

Winland (published by Koldozie, 1980) carried out regression analyses on sandstone samples to get out a relationship among porosity, permeability and pore throat size. He found the best fit at 35% mercury saturation. The Winland equation has the following form:

$$\text{Log } r_{35} = 0.732 + 0.588 \log K - 0.864 \log \Phi \text{.....(7)}$$

In the study reservoir, the equation that determined the best fit has the following form with $r^2 = 0.96$:

$$\text{Log } r_{60} = 1.043 + 0.29 \log K + 1.3 \log \Phi c \text{.....(8)}$$

The reservoir rock type based on Winland equation is illustrated in Figure 19. This figure indicates that three rock types are present. These rock types are meso, macro and mega rock types.

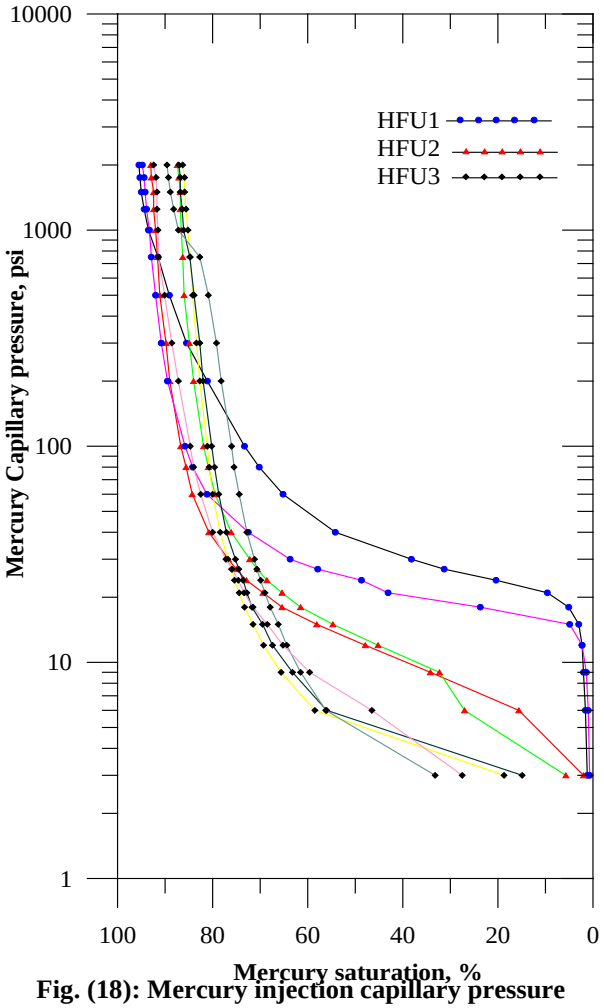

Fig. (18): Mercury injection capillary pressure for well B (HFU = hydraulic flow unit).

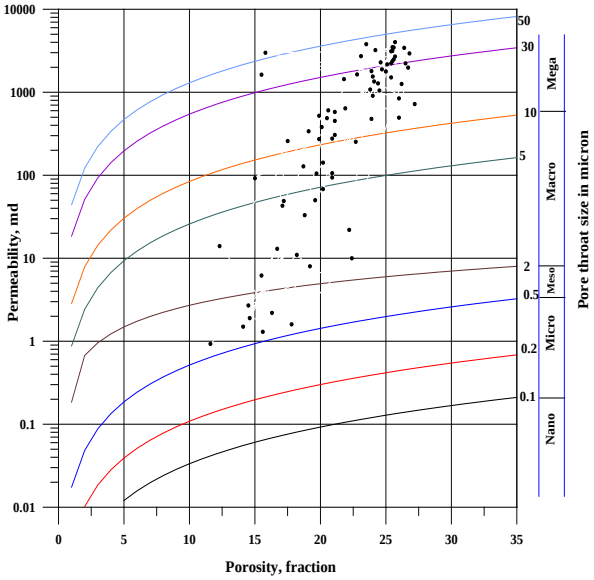

Fig. (19): Identification of reservoir rock type using Winland equation (Koldozie, 1980)

CONCLUSIONS

- The lower Miocene Nukhul Formation represents the first strata responded to the Gulf of Suez rifting.
- Facies and thickness of the Nukhul Formation vary from one place to another. The complete formation is missed in many wells due to the effect of fault movements post Shoab Ali Member. The complete section is usually encountered on the downthrown while on upthrown, the lower clastics section is usually missed.
- Shoab Ali Member can be divided into three units; each one was deposited in a different environment.
- The Nukhul clastics have a good to an excellent reservoir quality.
- Porosity plays the major controlling role in determination of permeability due to slightly diagenesis processes.
- Based on pore scale, Nukhul clastics reservoir is extremely heterogeneous.
- Three reservoir rock types as well as at least nine hydraulic flow units can be detected within the Nukhul clastics.
- Rock density is a good indicator for both porosity and permeability.

Acknowledgements

The Author is grateful to the Egyptian General Petroleum Corporation (EGPC) and Gulf of Suez Petroleum Company (GUPCO) for providing data.

REFERENCES

Bosworth, W., and K. McClay, 2001. Structural and stratigraphic evolution of the Gulf of Suez rift, Egypt: A synthesis. In; P.A. Ziegler, W. Cavazza, A.H.F. Roberston, S. Crasquin-Soleau (eds), Peri – Tethys Memoir 6: Peri – Tethyan Rift/ Wrench Basins and Passive Margins, p. 567-606.

Bosworth, W., P. Crerello, , R.D. Winn Jr, J. Steinmetz, 1998. Structure, sedimentation, and basin dynamics during rifting of the Gulf of Suez. In: Purser, B.H., Bosence, D.W.J.(Eds.), Sedimentation and Tectonics of Rift Basins: Red Sea – Gulf of Aden, pp. 78-96.

Dolson, J.C., O.E. Gendi, H. Charmy, M. Fathalla, and I. Gaafar, 1996. Gulf of Suez rift basin sequence models- part A, Miocene sequence stratigraphy and exploration significance in the greater October Field area, northern Gulf of Suez. 13th EGPC Exploration and Production Conference, v. 2, p. 227-241.

Dykstra, H. and R. L. Parsons, 1950. The Prediction of Oil Recovery in Waterflood. Seconday Recovey of Oil in the United States, 2nd ed. American Petroleum Institute (API), p. 160-174

Egyptian General Petroleum Corporation, EGPC, 1964. Oligocene and Miocene rock- stratigraphy of the Gulf of Suez region, report of the Stratigraphic Committee. Egyptian General Petroleum Corporation, 142 p.

Egyptian General Petroleum Corporation, EGPC, 1996. Gulf of Suez oil fields (A comprehensive overview), 736 pp.

El Sharawy, M.S., 2006. Seismic and well log data as an aid for evaluating oil and gas reservoirs in the southern part of the Gulf of Suez, Egypt. PhD dissertation, Mansoura University, Egypt, 265 p.

Evans, A.L., 1988. Neogene tectonic and stratigraphic events in the Gulf of Suez area, Egypt. Tectonophysics 153, 235-247.

Garfunkel, Z., Bartov, Y., 1977. The tectonics of the Suez rift. Geological Survey of Israel Bulletin 71, 45 pp.

Gunter G, J. Finneran, D. Hartmann, J. Miller, 1997. Early determination of reservoir flow units using an integrated petrophysical method: SPE Paper 38679, p 8

Haq, B.U., J. Hardenbol, , P.R. Vail, 1987. Chronology of fluctuating sea levels since the Triassic. Science 235, 1156 – 1167.

Jackson C, R. Gawthorpe, I. Sharp, 2006. Style and sequence of deformation during extensional fault-propagation folding: examples from the Hammam Faraun and El-Qaa fault blocks, Suez Rift, Egypt: Journal of Structural Geology 28(3): 519-535

Kolodzie, S., 1980. The analysis of pore throat size and the use of the Waxman – Smits equation to determine OOIP in the Spindle field, Colorado. SPE, 55th Annual Fall Technical Conference, Paper 9382, p. 2-4.

McClay, K.R., G.J. Nichols, S.M. Khalil, M. Darwish, W. Bosworth, 1998. Extensional tectonics and sedimentation, Eastern Gulf of Suez, Egypt: In: Purser, B.H., Bosence, D.W.J.(Eds.), Sedimentation and Tectonics of Rift Basins: Red Sea – Gulf of Aden, pp. 224-238.

Montenat, C., P. Ott d'Estevou, B. Purser,1986. Tectonic and sedimentary evolution of the Gulf of Suez and the northwestern Red Sea: a review. In: C. Montenat (Ed.), Geological studies of the Gulf of Suez, northwestern Red Sea coasts, tectonic and sedimentary evolution of Neogene rift: Documents et Travaux Institut Geologique Albert de Lapparent 10, 7-18.

Montenat, C., P. Ott d'Estevou, B.H. Purser, P. Burollet, J.J. Jarrige, F. Orszag-Sperber, E. Philobbos, J.C. Plaziat, P. Prat, J.P. Richert, N. Roussel, J.P. Thiriet, 1988. Tectonic and sedimentary evolution of the Gulf of Suez and

the northwestern Red Sea. Tectonophysics 153, 161-177.

Montenat, C., P. tt d'Estevou, J.J. arrige, J.P. ichert, 1998. Rift development in the Gulf of Suez and the northwestern Red Sea: structural aspects and related sedimentary processes, In: B.H. Purser and Bosence, D.W.J.(Eds.), Sedimentation and Tectonics of Rift Basins: Red Sea – Gulf of Aden, 98-116.

Morris, R. L., and W. P. Biggs, 1967. Using log-derived values of water saturation and porosity: Society of Professional Well Log Analysts Annual Logging Symposium, 26 p.

Moustafa, A., 2002. Controls on the geometry of transfer zones in the Gulf of Suez and Red Sea: implications for the structural geometry of rift systems: AAPG Bulletin 86 (6): 979-1002

Neal, J., D. Risch, and P. Vail, 1993. Sequence stratigraphy- a global theory for local success. Oilfield Review 5, no. 1, January, p. 51-62.

Patton, T.L., A.R. Moustafa, R.A. Nelson, A.S. Abdine,1994. Tectonic evolution and structural setting of the Suez rift. In: Landon, S.M. (Ed.), Interior rift basins: AAPG Memoir 59, 9-55.

Plaziat, J.C., C. Montenat, P. Barrier, M.C. Jania, F. Orszag-Sperber, E. Philobbos, 1998. Stratigraphy of the Egyptian synrift deposits: correlations between axial and peripheral sequences of the northwestern Red Sea and Gulf of Suez and their relations with tectonics eustacy. In: Purser, B.H., Bosence, D.W.J.(Eds.), Sedimentation and Tectonics of Rift Basins: Red Sea – Gulf of Aden, pp. 211-222.

Ramzy, M., B. Steer, F. Abu Shadi, M. Schlorholtz, J.Mika, J. Dolson, and M. zinger, 1996. Gulf of Suez rift basin sequence models- part B, Miocene sequence stratigraphy and exploration significance in the central and southern Gulf of Suez. 13th EGPC Exploration and Production Conference, v. 2, p. 242-254.

Richardson, M., M.A. Arthur, 1988. The Gulf of Suez-northern Red Sea Neogene rift: a quantitive basin analysis. Marine and Petroleum Geology 5, August, 247 – 270.

Saoudi,A., B. Kalil, 1984. Distribution and hydrocarbon potential of Nukhul sediments in the Gulf of Suez. 7th EGPC Exploration Seminar.

Salem, H.S., G.V. Chilingarian, 1999. The cementation factor of Archie's equation for shaly sandstone reservoirs. Journal of Petroleum Science and Engineering, 23, 1999, P. 83–93.

Schlumberger, 1982. Essentials of NGS interpretation.

Timur, A., 1968. An investigation of permeability, porosity, and residual water saturation relationships. Transactions of the SPWLA, 9th Annual Logging Symposium, paper J, 18 p.

Winn Jr., R.D., P.D. Crevello, , W. Bosworth, 2001. Lower Miocene Nukhul Formation, Gebel el Zeit, Egypt: Model for structural control on early synrift strata and reservoirs, Gulf of Suez. AAPG Bulletin 75, 1871-1890.

Wilson, P., R. Gawthorpe, D. Hodgetts, F. Rarity, I. Sharp, 2009. Geometry and architecture of faults in a syn-rift normal fault array: The Nukhul half-graben, Suez rift, Egypt: Journal Of Structural Geology 31: 759-775